

Forward - Backward Greedy Algorithms for Atomic Norm Regularization

Nikhil Rao Parikshit Shah Stephen Wright
University of Wisconsin - Madison

Abstract—In many signal processing applications, the aim is to reconstruct a signal that has a simple representation with respect to a certain basis or frame. Fundamental elements of the basis known as “atoms” allow us to define “atomic norms” that can be used to formulate convex regularizations for the reconstruction problem. Efficient algorithms are available to solve these formulations in certain special cases, but an approach that works well for general atomic norms, both in terms of speed and reconstruction accuracy, remains to be found. This paper describes an optimization algorithm called CoGenT that produces solutions with succinct atomic representations for reconstruction problems, generally formulated with atomic-norm constraints. CoGenT combines a greedy selection scheme based on the conditional gradient approach with a backward (or “truncation”) step that exploits the quadratic nature of the objective to reduce the basis size. We establish convergence properties and validate the algorithm via extensive numerical experiments on a suite of signal processing applications. Our algorithm and analysis also allow for inexact forward steps and for occasional enhancements of the current representation to be performed. CoGenT can outperform the basic conditional gradient method, and indeed many methods that are tailored to specific applications, when the enhancement and truncation steps are defined appropriately. We also introduce several novel applications that are enabled by the atomic-norm framework, including tensor completion, moment problems in signal processing, and graph deconvolution.

I. INTRODUCTION

Minimization of a convex loss function with a constraint on the “simplicity” of the solution has found widespread applications in communications, machine learning, image processing, genetics, and other fields. While exact formulations of the simplicity requirement are often intractable, it is sometimes possible to devise tractable formulations via convex relaxation that are (nearly) equivalent. Since these formulations differ so markedly across applications, a principled and unified convex heuristic for different notions of simplicity

has been proposed using notions of *atoms* and *atomic norms* [1]. Atoms are fundamental basis elements of the representation of a signal, chosen so that “simplicity” equates to “representable in terms of a small number of atoms.” We list several applications, describing for each application a choice of atoms that captures the concept of simplicity for those applications.

A sparse signal x may be represented as $x = \sum_{j \in \mathcal{S}} c_j e_j$, where the e_j are the standard unit vectors and \mathcal{S} captures the support of x . One can view the set $\{\pm e_j\}$ as *atoms* that constitute the signal, and the convex hull of these atoms is a set of fundamental importance called the *atomic-norm ball*. The operation of inflation/deflation of the atomic norm ball induces a norm (the *atomic norm*), which serves as an effective regularizer (see Sec. I-A). The atomic set $\{\pm e_j, j = 1, 2, \dots, p\}$ induces the ℓ_1 norm [2], which is well known to be an effective regularizer for sparsity. However, this idea can be generalized. For instance, the atomic norm induced by the convex hull of all unit-rank matrices is the nuclear norm, often used as a heuristic for rank minimization [3], [4]. Other novel applications of the atomic-norm framework include the following.

- **Group-norm-constrained multitask learning** problems with group- ℓ_2 norms [5]–[7] or group- ℓ_∞ norms [8]–[10] have as atoms unit Euclidean balls and unit ℓ_∞ -norm balls, respectively, restricted to specific groups of variables.
- **Group lasso with overlapping groups** arises from applications in genomics, image processing, and machine learning [5], [7]. It is shown in [11] that the sum of ℓ_2 norms of overlapping groups of variables is an atomic norm.
- **Moment problems**, which arise in applications such as radar, communications, seismology, and sensor arrays, have an atomic set which is uncountably infinite [12]. Each atom is a trigonometric moment sequence of an atomic measure supported on the unit interval [12]. This methodology can be extended to signal classes such as Bessel functions,

Copyright (c) 2015 IEEE. Personal use of this material is permitted. However, permission to use this material for any other purposes must be obtained from the IEEE by sending a request to pubs-permissions@ieee.org.

Gaussians, and wavelets.

- **Group testing on graphs** and network tomography finds widespread applications in sensor, computer, social, and biological networks [7], [13]. It is typically required to identify a set of faulty edges/nodes from measurements that are based on the known structure of the graph. Each atom can be defined as a subset of nodes or edges in the graph.
- **Hierarchical norms** arise in topic modeling [14], climate and oceanology applications [15], and fMRI data analysis [16]. The atoms here are hybrids of group-sparse and sparse atoms.
- **OSCAR-regularized** problems use an octagonal penalty to simultaneously identify a sparse set of pairwise correlated variables [17]. The authors in [18] show that it can be cast as an atomic-norm-regularized problem. In two dimensions, the atoms are the signed canonical basis vectors, and vectors with equal magnitude entries.
- **Tensor Completion:** Signals modeled as tensors have recently enjoyed renewed interest in machine learning [19]. We consider here the case of symmetric, orthogonally decomposable, and low-symmetric-rank tensors, in which the atoms are unit-rank symmetric tensors.
- **Deconvolution** is the problem of splitting a signal $z = x + y$ into two components that are succinct with respect to different sets of atoms [20]. Typical cases include the atomic sets being sparse and low-rank [21], sparse in the canonical and discrete cosine transform (DCT) bases, and sparse and group-sparse [22].

We present a general method called CoGenT (for “Conditional Gradient with Enhancement and Truncation”) that can be applied to general atomic-norm-regularized formulations, including formulations of the applications discussed above. CoGenT minimizes a least-squares loss function that measures the difference between predictions based on signal representation and the actual observations, subject to a “simplicity” constraint on the signal, imposed via an atomic norm. Besides its generality, novel aspects of CoGenT include (a) introduction of *enhancement steps* at each iteration to improve solution fidelity, (b) introduction of efficient *backward steps* that improve the quality of the reconstruction, (c) introduction of the notion of *inexactness* in the forward step.

A. Preliminaries and Notation

We assume the existence of a known atomic set \mathcal{A} and an unknown signal \mathbf{x} in some “ambient” space, where \mathbf{x}

is a superposition of a small number of atoms from \mathcal{A} . (We emphasize that the set of atoms need not be finite.) We assume further that the set \mathcal{A} is symmetric about the origin, that is, $\mathbf{a} \in \mathcal{A} \Rightarrow -\mathbf{a} \in \mathcal{A}$. The representation of \mathbf{x} as a conic combination of atoms $\mathbf{a} \in \mathcal{A}_t$ in a subset $\mathcal{A}_t \subset \mathcal{A}$ is written as follows:

$$\mathbf{x} = \sum_{\mathbf{a} \in \mathcal{A}_t} c_{\mathbf{a}} \mathbf{a}, \quad \text{with } c_{\mathbf{a}} \geq 0 \text{ for all } \mathbf{a} \in \mathcal{A}_t. \quad (1)$$

where the $c_{\mathbf{a}}$ are scalar coefficients. We write

$$\mathbf{x} \in \text{co}(\mathcal{A}_t, \tau), \quad (2)$$

for some given $\tau \geq 0$, if it is possible to represent the vector \mathbf{x} in the form (1), with the additional constraint

$$\sum_{\mathbf{a} \in \mathcal{A}_t} c_{\mathbf{a}} \leq \tau. \quad (3)$$

We use \mathbf{A}_t to denote a linear operator which maps the coefficient vector c (with cardinality $|\mathcal{A}_t|$) to a vector in the ambient space, using the vectors in \mathcal{A}_t , that is,

$$\mathbf{A}_t c := \sum_{\mathbf{a} \in \mathcal{A}_t} c_{\mathbf{a}} \mathbf{a}. \quad (4)$$

Since there is a one-to-one relationship between \mathcal{A}_t and the linear operator \mathbf{A}_t , we use the notation (4) more often, and sometimes slightly abuse terminology by referring to \mathbf{A}_t as the “basis” at iteration t . We sometimes refer to the “columns” of \mathbf{A}_t , by which we mean the elements of the corresponding basis \mathcal{A}_t . The *atomic norm* [1] is the gauge functional induced by \mathcal{A} :

$$\|\mathbf{x}\|_{\mathcal{A}} := \inf\{t > 0 : \mathbf{x} \in t(\text{conv}(\mathcal{A}))\}, \quad (5)$$

where $\text{conv}(\cdot)$ denotes the convex hull of a collection of points. Equivalently, we have

$$\|\mathbf{x}\|_{\mathcal{A}} := \inf \left\{ \sum_{\mathbf{a} \in \mathcal{A}} c_{\mathbf{a}} : \mathbf{x} = \sum_{\mathbf{a} \in \mathcal{A}} c_{\mathbf{a}} \mathbf{a}, \quad c_{\mathbf{a}} \geq 0 \right\}. \quad (6)$$

Given a representation (1), the sum of coefficients in (3) is an *upper bound* on the atomic norm $\|\mathbf{x}\|_{\mathcal{A}}$. The dual atomic norm is given by

$$\|\mathbf{x}\|_{\mathcal{A}}^* = \sup_{\|\mathbf{u}\|_{\mathcal{A}} \leq 1} \langle \mathbf{u}, \mathbf{x} \rangle. \quad (7)$$

The dual atomic norm is key to our approach — the atom selection step in CoGenT (as in the basic CG approach) amounts to choosing the argument that achieves the supremum in (7), for a particular choice of \mathbf{x} .

CoGenT solves the convex optimization problem:

$$\min_{\mathbf{x}} f(\mathbf{x}) := \frac{1}{2} \|\mathbf{y} - \Phi \mathbf{x}\|_2^2 \quad \text{s.t.} \quad \|\mathbf{x}\|_{\mathcal{A}} \leq \tau, \quad (8)$$

where $\mathbf{y} = \Phi \mathbf{x} + \mathbf{w}$ corresponds to observed measurements, with noise vector \mathbf{w} . The regularizing constraint

on the atomic norm of \mathbf{x} enforces “simplicity” with respect to the chosen atomic set. Efficient algorithms are known for this problem when the atoms are standard unit vectors $\pm e_j$ (for which the atomic norm is the ℓ_1 norm) [23]–[25] and rank-one matrices (for which the atomic norm is the nuclear norm) [26], [27]. CoGenT targets the general formulation (8), opening up a suite of new applications with rigorous convergence guarantees and state-of-the-art empirical performance.

We remark that while (8) is a convex formulation, efficient algorithms for solving it are not known in full generality. Indeed, computation of the atomic norm is itself a difficult operation in some applications. From an optimization perspective, interior point methods are often impractical, being either difficult to formulate or too slow for large-scale instances. By contrast, first-order greedy methods are popular in high dimensional signal recovery settings because of their computational efficiency, scalability to large datasets, and interesting global rate-of-convergence properties. They have found widespread use in large scale machine learning and signal processing applications [28]–[34].

B. Past Work: Conditional Gradient Method

A conditional gradient (CG) algorithm for (8) was introduced in [30]. This greedy approach is often known as “Frank-Wolfe” after the authors who proposed it in the 1950s [35]. At each iteration, the CG algorithm finds the atom that optimizes a first-order approximation to the objective over the feasible region, and adds this atom to the basis for the solution. Each iteration of CoGenT performs a “forward step” of this type, and it is this step that drives the convergence theory, which is similar to that of standard CG methods [29], [30], although some use a different treatment of inexactness in the choice of search direction. For a detailed review of the CG method, see [28] and references therein.

Although greedy methods require more iterations than such prox-linear methods as SpaRSA [23], FISTA [36], and Nesterov’s accelerated gradient method [37], each iteration is typically less expensive. For example, in matrix completion applications, prox-linear methods require computation of an SVD of a matrix [38] (or at least a substantial part of it), while CG requires only the computation of the top singular vector pair. In other applications, such as structural SVM [39], CG schemes are the only practical way to solve the optimization formulation. Latent group lasso [7] can be extended to perform regression on very large signals by employing a “replication” strategy, but as the amount of group overlap increases, prox-linear methods quickly become memory

intensive. CG offers a scalable alternative for solving problems of this form. The procedure to choose each new atom has a linear objective, as opposed to the quadratic program required to perform projection steps in prox-linear methods. The linear subproblem is often easier to solve, and it need only be solved approximately to retain convergence guarantees [28], [32].

C. Backward (Truncation) Steps

In signal processing applications, one is interested not only in minimizing the loss function, but also in the “simplicity” of the solutions. For example, when the solution corresponds to the wavelet coefficients of an image, sparsity of the representation is key to its usefulness as a compact representation. In this regard, the basic CG and indeed all greedy schemes suffer from a significant drawback: Atoms added at some iterations may be superseded by others added at later iterations, and ultimately may not contribute much to reducing the loss function. By the time the loss function has been reduced to an acceptable level, the basis may contain many such atoms of dubious value, thus detracting from the quality of the solution.

Backward steps in CoGenT allow atoms to be removed from the basis when they are found to be unhelpful in reducing the objective. We define this step in a flexible way, the only requirement being that it does not degrade the objective function too greatly in comparison to the gain that was obtained at the most recent “forward” iteration. We discuss two possible implementations of this step — Algorithms 2 and 3 — in the next section.

The “away steps” analyzed in [40] are closely related to one of our backward/truncation strategies. However, the primary consideration in [40] remains improvement in the objective value, rather than sparsity: Away steps are taken only when, to first order, they promise greater decrease in the objective than the most recently calculated forward step. Because we seek sparse solutions, we allow backward / truncation steps to be taken in more general circumstances, even when slight increases in the objective occur. We note that the “away steps” of [40] differ from those in the original proposal of Wolfe [41], which may *increase* the size of the basis.

Forward-backward greedy schemes for ℓ_1 constrained minimization have been considered previously in [42]–[45]. These methods build on the Orthogonal Matching Pursuit (OMP) algorithm [24], and cannot be readily extended to the general setting (8).

D. Enhancement (Reoptimization) Steps

The enhancement / reoptimization step in CoGenT takes the current basis and seeks a new set of

coefficients in the representation (4) that reduces the objective while satisfying the norm constraint. (A “full correction” step of this type was described in [28].) The step is implemented as a linear least-squares objective over the positive orthant of the ℓ_1 norm ball. CoGenT solves it with a projected gradient method, using a warm start based on the current set of coefficients. Since projected gradient is a descent method that maintains feasibility, it can be stopped after any number of iterations, without prejudice to the convergence rate of CoGenT. The use of projected gradient allows “interpolation” between the basic CG strategy of adding the new atom with minimal adjustment of coefficients, and complete reoptimization over the expanded basis.

E. Outline of the Paper

The rest of the paper is organized as follows. We specify CoGenT in the next section, describing different variants of the backward step that promote parsimonious solutions. In Section III, we state convergence results, deferring proofs to an appendix. Section IV describes the application of CoGenT to a number of existing applications, and compares it to various other methods that have been proposed for these applications. In Section V, we apply CoGenT for a variety of *new* applications, for which current methods, if they exist at all, do not scale well to large data sets. In Section VI we extend our algorithm to deal with deconvolution problems.

The authors presented a nascent version of CoGenT with a few experimental results in [46]. The algorithm in its current form was first presented in [47]. This paper explains CoGenT in full detail, provides theoretical convergence guarantees in both exact and approximate settings, and extensive empirical results.

II. ALGORITHM

CoGenT is specified in Algorithm 1. Its three major elements — the forward (conditional gradient) step, the backward (truncation) step, and the enhancement (reoptimization) step — have been discussed in Section I. We note that these three steps are constructed so that the iterates at each step are feasible (that is, $\|\mathbf{x}_t\|_{\mathcal{A}} \leq \tau$). We make further notes in this section about alternative implementations of these three steps.

The forward step (Step 4) is equivalent to solving an approximation to (8) based on a linearization of f around the current iterate. Specifically, it is easy to show that $\tau\mathbf{a}_t$ solves the following problem:

$$\min_{\mathbf{x}} f(\mathbf{x}_t) + \langle \nabla f(\mathbf{x}_t), \mathbf{x} - \mathbf{x}_t \rangle \quad \text{s.t.} \quad \|\mathbf{x}\|_{\mathcal{A}} \leq \tau.$$

Algorithm 1 CoGenT: Conditional Gradient with Enhancement and Truncation

- 1: **Input:** Linear oracle for \mathcal{A} , bound τ , threshold parameter $\eta \in (0, 1/2]$;
 - 2: **Initialize,** $\mathbf{a}_0 \in \mathcal{A}$, $t \leftarrow 0$, $\mathbf{A}_0 \leftarrow [\mathbf{a}_0]$, $c_0 \leftarrow [\tau]$, $\mathbf{x}_0 \leftarrow \mathbf{A}_0 c_0$;
 - 3: **repeat**
 - 4: $\mathbf{a}_{t+1} \leftarrow \arg \min_{\mathbf{a} \in \mathcal{A}} \langle \nabla f(\mathbf{x}_t), \mathbf{a} \rangle$; {FORWARD}
 - 5: $\tilde{\mathbf{A}}_{t+1} \leftarrow [\mathbf{A}_t \quad \mathbf{a}_{t+1}]$;
 - 6: $\gamma_{t+1} \leftarrow \arg \min_{\gamma \in [0, 1]} f(\mathbf{x}_t + \gamma(\tau\mathbf{a}_{t+1} - \mathbf{x}_t))$; {LINE SEARCH}
 - 7: $\tilde{c}_{t+1} \leftarrow [(1 - \gamma_{t+1})c_t \quad \gamma_{t+1}\tau\mathbf{a}_{t+1}]$;
 - 8: **Optional:** Approximately solve $\tilde{c}_{t+1} \leftarrow \arg \min_{c_{t+1}} f(\tilde{\mathbf{A}}_{t+1}c_{t+1})$ s.t. $\|c_{t+1}\|_1 \leq \tau$, $c_{t+1} \geq 0$ with the output from Step 7 as a warm start; {ENHANCEMENT}
 - 9: $\tilde{\mathbf{x}}_{t+1} = \tilde{\mathbf{A}}_{t+1}\tilde{c}_{t+1}$;
 - 10: Threshold $F_{t+1} := \eta f(\mathbf{x}_t) + (1 - \eta)f(\tilde{\mathbf{x}}_{t+1})$;
 - 11: $[\mathbf{A}_{t+1}, c_{t+1}, \mathbf{x}_{t+1}] = \text{TRUNCATE}(\tilde{\mathbf{A}}_{t+1}, \tilde{c}_{t+1}, \tau, F_{t+1})$; {BACKWARD}
 - 12: $t \leftarrow t + 1$;
 - 13: **until convergence**
 - 14: **Output:** \mathbf{x}_t
-

(A simple argument reveals that the minimizer of this problem is attained by $\tau\mathbf{a}$, where \mathbf{a} is an atom.) We assume the knowledge of a linear oracle that, given a set of atoms \mathcal{A} , returns the solution of $\arg \min_{\mathbf{a} \in \mathcal{A}} \langle \mathbf{v}, \mathbf{a} \rangle$ for a vector \mathbf{v} . For most applications of interest, the linear oracle can be calculated efficiently.

The line search of Step 6 can be performed exactly, because of the quadratic objective in (8). We obtain

$$\gamma_{t+1} = \min \left\{ \frac{\langle \mathbf{y} - \Phi\mathbf{x}_t, \Phi\mathbf{v} \rangle}{\|\Phi\mathbf{v}\|^2}, 1 \right\}, \quad \mathbf{v} := \tau\mathbf{a}_{t+1} - \mathbf{x}_t.$$

As mentioned in Section I-D, Step 8 can be solved using projected gradient methods. Projection onto the ℓ_1 ball can be performed efficiently [48], in $O(n_{t+1} \log(n_{t+1}))$ operations, where n_{t+1} is the number of elements in the current basis \mathcal{A}_{t+1} . Each step of projected gradient yields descent in the objective, so we can terminate the process before performing full reoptimization over the current basis. Although the enhancement step is optional, we include it in all the experiments described in Section IV.

We now discuss two options for performing the backward (truncation) step (Step 11), whose purpose is to compactify the representation of \mathbf{x}_t , without degrading

the objective more than a specified amount. The parameter η defines a sufficient decrease criterion that the modified solution needs to satisfy. A value of η closer to its upper bound will yield more frequent removal of atoms and hence a sparser solution, at the expense of more modest progress per iteration.

Our first implementation of the truncation step (see Algorithm 2) seeks to purge one or more elements from the expanded basis \mathbf{A}_{t+1} , using a quadratic prediction of the effect of removal of each atom. Removal of an atom \mathbf{a} (and hence the corresponding coefficient $c_{\mathbf{a}}$) from the current iterate $\tilde{\mathbf{x}}_{t+1}$ in Step 4 of Algorithm 2 results in the following change to the objective:

$$\begin{aligned} & f(\tilde{\mathbf{x}}_{t+1} - c_{\mathbf{a}}\mathbf{a}) \\ &= f(\tilde{\mathbf{x}}_{t+1}) - c_{\mathbf{a}}\langle \nabla f(\tilde{\mathbf{x}}_{t+1}), \mathbf{a} \rangle + \frac{1}{2}c_{\mathbf{a}}^2\|\Phi\mathbf{a}\|_2^2. \end{aligned} \quad (9)$$

(We have assumed that $c_{\mathbf{a}}$ is the coefficient of \mathbf{a} in the current representation of $\tilde{\mathbf{x}}_{t+1}$.) The scalar quantities $\|\Phi\mathbf{a}\|_2^2$ can be computed efficiently and stored as soon as each atom \mathbf{a} enters the current basis \mathbf{A}_t , so the main cost in evaluating this criterion is in forming the inner product $\langle \nabla f(\tilde{\mathbf{x}}_{t+1}), \mathbf{a} \rangle$. Having chosen a candidate atom that optimizes the degradation in f , we can simply remove it from the basis and set its coefficient to zero. Alternatively, we can reoptimize over the remaining elements (Step 6 in Algorithm 2), possibly using the same projected gradient approach as in Step 8 of Algorithm 1, and test to see whether the updated value of f still falls below the threshold F_{t+1} . The projected gradient method in this case will be solving the following optimization program:

$$\hat{c}_{t+1} = \arg \min_c f(\hat{\mathbf{A}}_{t+1}c) \quad \mathbf{s.t.} \quad c \geq 0, \|c\|_1 \leq \tau.$$

Atom removal may be repeated in Algorithm 2 as long as the successively updated objective stays below the threshold F_{t+1} .

Our second implementation of the truncation step allows for a wholesale redefinition of the current basis, seeking a new, smaller basis and a new set of coefficients such that the objective value is not degraded too much. The approach is specified in Algorithm 3, and is what we use for the matrix and tensor completion experiments later in the paper. It is motivated by the observation that atoms added at early iterates contain spurious components, which may not be canceled out by atoms added at later iterations. This phenomenon is apparent in matrix completion, where the number of atoms (rank-one matrices) generated by the procedure above is often considerably larger than the rank of the target matrix. For this application, we implement step 2 of Algorithm 3

Algorithm 2 : TRUNCATE($\tilde{\mathbf{A}}_{t+1}, \tilde{c}_{t+1}, \tau, F_{t+1}$)

- 1: **Input:** Current basis $\tilde{\mathbf{A}}_{t+1}$, coefficient vector \tilde{c}_{t+1} , iterate $\tilde{\mathbf{x}}_{t+1} = \tilde{\mathbf{A}}_{t+1}\tilde{c}_{t+1}$; bound τ ; threshold F_{t+1} ;
 - 2: continue $\leftarrow 1$;
 - 3: **while** continue = 1 **do**
 - 4: $\hat{\mathbf{a}}_{t+1} \leftarrow \arg \min_{\mathbf{a} \in \tilde{\mathbf{A}}_{t+1}} f(\tilde{\mathbf{x}}_{t+1} - c_{\mathbf{a}}\mathbf{a})$
 - 5: $\hat{\mathbf{A}}_{t+1} \leftarrow \tilde{\mathbf{A}}_{t+1} \setminus \{\hat{\mathbf{a}}_{t+1}\}$;
 - 6: Find $\hat{c}_{t+1} \geq 0$ with $\|\hat{c}_{t+1}\|_1 \leq \tau$ such that $f(\hat{\mathbf{A}}_{t+1}\hat{c}_{t+1}) \leq f(\tilde{\mathbf{x}}_{t+1} - (\tilde{c}_{\hat{\mathbf{a}}_{t+1}})_{t+1}\hat{\mathbf{a}}_{t+1})$;
 - 7: **if** $f(\hat{\mathbf{A}}_{t+1}\hat{c}_{t+1}) \leq F_{t+1}$ **then**
 - 8: $\hat{\mathbf{A}}_{t+1} \leftarrow \hat{\mathbf{A}}_{t+1}$;
 - 9: $\tilde{\mathbf{x}}_{t+1} \leftarrow \hat{\mathbf{A}}_{t+1}\hat{c}_{t+1}$;
 - 10: $\tilde{c}_{t+1} \leftarrow \hat{c}_{t+1}$;
 - 11: **else**
 - 12: continue $\leftarrow 0$;
 - 13: **end if**
 - 14: **end while**
 - 15: $\mathbf{A}_{t+1} \leftarrow \hat{\mathbf{A}}_{t+1}$; $\mathbf{x}_{t+1} \leftarrow \tilde{\mathbf{x}}_{t+1}$; $c_{t+1} \leftarrow \tilde{c}_{t+1}$;
 - 16: **Output:** Possibly reduced basis \mathbf{A}_{t+1} , coefficient vector $c_{t+1} \geq 0$, and iterate \mathbf{x}_{t+1} .
-

by forming a singular value decomposition of the matrix represented by the latest iterate $\tilde{\mathbf{x}}_{t+1}$, and defining a new basis $\hat{\mathbf{A}}_{t+1}$ to be a low-rank matrix that corresponds to the largest singular values. These singular values would then form the new coefficient vector \hat{c}_{t+1} , and the new iterate \mathbf{x}_{t+1} would be defined in terms of just these singular values and singular vectors. The computational work required for such a step would be comparable with one iteration of the popular singular value thresholding (SVT) approach [38] for matrix completion, which also requires calculation of the leading singular values and singular vectors.

We conclude this section by discussing practical stopping criteria for Algorithm 1. As we show in Section III, CoGenT is guaranteed to converge to an optimum, and the objective is guaranteed to decrease at each iteration. We therefore use the following termination criteria:

$$\frac{f(\mathbf{x}_{t-1}) - f(\mathbf{x}_t)}{f(\mathbf{x}_{t-1})} \leq \text{tol},$$

where tol is a small user-defined parameter.

III. CONVERGENCE RESULTS

Convergence properties for CoGenT are stated here, with proofs appearing in the appendix. Sublinear convergence of CoGenT (Theorem III.1) follows from a mostly familiar argument.

Algorithm 3 TRUNCATE($\tilde{\mathbf{A}}_{t+1}, \tilde{\mathbf{c}}_{t+1}, \tau, F_{t+1}$)

- 1: **Input:** Current basis $\tilde{\mathbf{A}}_{t+1}$, coefficient vector $\tilde{\mathbf{c}}_{t+1}$, iterate $\tilde{\mathbf{x}}_{t+1} = \tilde{\mathbf{A}}_{t+1}\tilde{\mathbf{c}}_{t+1}$; bound τ ; threshold F_{t+1} ;
 - 2: Find alternative basis $\hat{\mathbf{A}}_{t+1}$ and coefficients $\hat{\mathbf{c}}_{t+1} \geq 0$ such that $\#\text{columns}(\hat{\mathbf{A}}_{t+1}) < \#\text{columns}(\tilde{\mathbf{A}}_{t+1})$, $\|\hat{\mathbf{c}}_{t+1}\|_1 \leq \tau$;
 - 3: **if** $f(\hat{\mathbf{A}}_{t+1}\hat{\mathbf{c}}_{t+1}) \leq F_{t+1}$ **then**
 - 4: $\mathbf{A}_{t+1} \leftarrow \hat{\mathbf{A}}_{t+1}$; $\mathbf{x}_{t+1} \leftarrow \hat{\mathbf{A}}_{t+1}\hat{\mathbf{c}}_{t+1}$; $\mathbf{c}_{t+1} \leftarrow \hat{\mathbf{c}}_{t+1}$;
 - 5: **else**
 - 6: $\mathbf{A}_{t+1} \leftarrow \tilde{\mathbf{A}}_{t+1}$; $\mathbf{x}_{t+1} \leftarrow \tilde{\mathbf{x}}_{t+1}$; $\mathbf{c}_{t+1} \leftarrow \tilde{\mathbf{c}}_{t+1}$;
 - 7: **end if**
 - 8: **Output:** Possibly reduced basis \mathbf{A}_{t+1} , coefficient vector $\mathbf{c}_{t+1} \geq 0$, and iterate \mathbf{x}_{t+1} .
-

Theorem III.1. Consider the convex optimization problem (8), and let \mathbf{x}^* be a solution of (8). Let $\eta \in (0, 1/2]$. Then the sequence of function values $\{f(\mathbf{x}_t)\}$ generated by CoGenT converges to $f^* = f(\mathbf{x}^*)$ with

$$f(\mathbf{x}_T) - f^* \leq \frac{\bar{C}}{T+1}, \quad \text{for all } T \geq 1, \quad (10)$$

where

$$\begin{aligned} \bar{C}_1 &:= \eta D + 2(1-\eta)LR^2\tau^2, \\ \bar{C} &:= \frac{2\bar{C}_1^2}{(1-\eta)(\bar{C}_1 - LR^2\tau^2)} > 0, \\ L &:= \|\Phi^T \Phi\|, \\ D &:= f(\mathbf{x}_0) - f(\mathbf{x}^*), \\ R &:= \max_{\mathbf{a} \in \mathcal{A}} \|\mathbf{a}\|. \end{aligned}$$

When the true optimum \mathbf{x}^* lies in the interior of the set $\|\mathbf{x}\|_{\mathcal{A}} \leq \tau$, and when Φ has full row rank, the objective function becomes strongly convex and linear convergence results for the standard CG method apply to CoGenT as well [40], [49]. (We omit the formal statement and full proof of this result, since in most applications of interest, the solution will lie on the boundary of the atomic-norm ball.)

Similar convergence properties hold when the atom added in the forward step of Algorithm 1 is computed *approximately*¹. In place of the argmin in Step 4 of Algorithm 1, we have the following requirement on $\mathbf{a}_{t+1} \in \mathcal{A}$:

$$\langle \nabla f(\mathbf{x}_t), \tau \mathbf{a}_{t+1} - \mathbf{x}_t \rangle \leq (1-\omega) \min_{\mathbf{a} \in \mathcal{A}} \langle \nabla f(\mathbf{x}_t), \tau \mathbf{a} - \mathbf{x}_t \rangle \quad (11)$$

¹Approximately solving this step can be critical in making the approach practical for a wider variety of applications, as we see later.

where $\omega \in (0, 1/4)$ is a user-defined parameter. Unless \mathbf{x}_t is a solution, the right-hand side of this expression is negative, so this condition essentially requires us to find a solution of the subproblem with relative objective accuracy ω . If a tight lower bound for the minimum is available from duality, this condition can be checked in practice. This criterion requires the approximate solution to attain a fraction of at least $(1-\omega)$ of the duality gap, given by $-\min_{\mathbf{a} \in \mathcal{A}} \langle \nabla f(\mathbf{x}_t), \tau \mathbf{a} - \mathbf{x}_t \rangle$. It is similar in spirit to the inexact Newton method for nonlinear equations [50, pp. 277-279], which requires the approximate solution of the linearized model to achieve only a fraction of the decrease promised by exact solution of the model. A similar condition on the relative accuracy of the subproblem solution was used in [39, formula (12)] and [51, Appendix A].

For the relaxed definition (11) of \mathbf{a}_{t+1} , we obtain the following result.

Theorem III.2. Assume that the conditions of Theorem III.1 hold, but that the atom \mathbf{a}_{t+1} selected in Step 4 in Algorithm 1 satisfies the condition (11). Assume further than $\eta \in (0, 1/3)$ and $\omega \in (0, 1/4)$. Then we have

$$f(\mathbf{x}_T) - f^* \leq \frac{\tilde{C}}{T+1} \quad \text{for all } T \geq 1, \quad (12)$$

where

$$\begin{aligned} \tilde{C}_1 &:= (\eta + \omega(1-\eta))D + 2(1-\eta)LR^2\tau^2, \\ \tilde{C} &:= \frac{2\tilde{C}_1^2}{(1-\eta)[(1-\omega)\tilde{C}_1 - LR^2\tau^2]}, \end{aligned}$$

with L, R, τ, D defined as in Theorem III.1

IV. EXPERIMENTS: STANDARD APPLICATIONS IN SPARSE RECOVERY

CoGenT can be used to solve a variety of problems in signal processing and machine learning, as we show in the remainder of the paper. In all our experiments (including those in Section V), unless specified otherwise, we choose a random atom for initialization, and set the parameter η to 0.5. All times reported correspond to the time taken for the algorithm to begin its first iteration and “finish,” exhausting the specified maximum number of iterations or converging to the solution based on the tolerance value provided. Wherever available, we set τ to be the atomic norm of the true signal of interest, and for competing algorithms, supply the true value of the parameter required by the method (sparsity, rank, etc.). Finally, in all tables and figures, we use “CG” to refer to the variant of conditional gradient in which line search is used to find the optimal step size at each iteration.

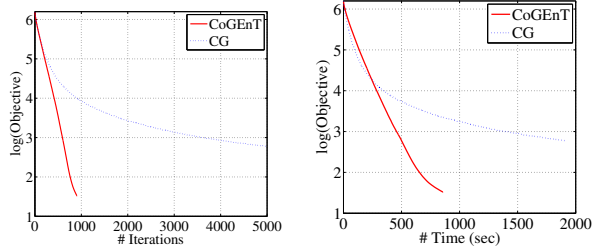


Fig. 1: Comparison between CoGenT and standard conditional gradient (CG).

A. Sparse Signal Recovery

We first start with the well known case of sparse signal recovery. We tested our method on the following formulation:

$$\hat{\mathbf{x}} = \arg \min_{\mathbf{x} \in \mathbb{R}^p} \|\mathbf{y} - \Phi \mathbf{x}\|_2^2 \quad \text{s.t.} \quad \|\mathbf{x}\|_1 \leq \tau. \quad (13)$$

The atoms in this case are the signed canonical basis vectors, and the atom selection step (Step 4 in Algorithm 1) reduces to the following:

$$\hat{i} = \arg \max_i |[\nabla f(\mathbf{x}_t)]_i|,$$

$$\mathbf{a}_{t+1} = -\text{sign}([\nabla f(\mathbf{x}_t)]_{\hat{i}}) \mathbf{e}_{\hat{i}}.$$

The above operation amounts to performing a sort, which can be done in $O(p \log(p))$ time. We consider a sparse signal \mathbf{x} of length $p = 20000$, with 5% of randomly set to nonzero values.² Setting $n = 5000$, we construct the $n \times p$ matrix Φ to have i.i.d. Gaussian entries, and corrupt the measurements with Gaussian noise (AWGN) of standard deviation $\sigma = 0.01$. In the formulation (13), we set $\tau = \|\mathbf{x}^*\|_1$, where \mathbf{x}^* is the chosen optimal signal.

To check the performance of CoGenT against the basic CG method, we run both methods for a maximum of 5000 iterations, with a stopping tolerance of 10^{-8} . Fig. 1 shows a graph of the logarithm of the function value vs iteration count (left) and logarithm of the function value vs wall clock time (right). On a per-iteration basis, CoGenT performs more operations than standard CG, but the use of backward steps yields faster reduction in the objective function value, resulting in better convergence, even when measured in terms of run time.

To compare and contrast the effect of various steps in CoGenT, we consider a length $p = 2000$ signal and obtain 600 Gaussian measurements, corrupted by

²Here and subsequently, the phrase “we randomly set coefficients to be nonzero” means that we select coefficients uniformly and assign them values from the normal distribution $\mathcal{N}(0, 1)$.

noise with $\sigma = 0.05$. We randomly set 5% of the coefficients of the target vector to nonzero values, and set $\tau = \|\mathbf{x}^*\|_1$ and $\text{tol} = 10^{-8}$, and allow a maximum of 1000 iterations. Table I compares the Normalized MSE $\|\mathbf{x}^* - \hat{\mathbf{x}}\|_2^2 / \|\mathbf{x}^*\|_2^2$ and the mean ℓ_1 error $\|\mathbf{x}^* - \hat{\mathbf{x}}\|_1 / p$ for various methods. The fully corrective variant [28] is only marginally better than CoGenT without truncation³, but more expensive since the enhancement step only solves the problem approximately. Also note the significant reduction in error once we add the truncation steps.

Method	NMSE $\times 100$	L1 Error $\times 100$
FW	5.848	0.954
FW _{full}	2.312	0.887
CG	3.993	0.682
CG _{En}	2.314	0.886
CoGenT	1.030	0.348

TABLE I: Performance comparison for different variants of the Frank Wolfe (Conditional Gradient) method and CoGenT. FW stands for the Frank Wolfe method with a step size of $\frac{2}{2+t}$, FW_{full} is the fully corrective variant, CG is the conditional gradient method with a line search for the step size. CG_{En} is CoGenT without the truncation step.

We now assess the influence of the enhancement step in CoGenT. To do so, we consider the recovery of a sparse signal of length 500, with 10% coefficients randomly set to nonzero values, with 200 noisy ($\sigma = 0.05$) Gaussian measurements. For this experiment, we chose the convergence criterion to be the NMSE, set the maximum allowed iterations in CoGenT to be 10000, and $\tau = \|\mathbf{x}^*\|_1$. We vary the number of projected gradient steps in the enhancement phase, to quantify the tradeoff between the time required to solve the enhancement subproblems and the reduction in the number of CoGenT iterations. Fig. 2 plots both final NMSE and total time taken vs the maximum number of steps allowed in the enhancement subproblems, averaged over 15 trials. (Zero enhancement iterations corresponds to standard CG.) This plot shows that the best overall solution times are obtained from a moderate-accuracy solution of the enhancement step, with a maximum of about 10 to 15 gradient projection iterations. (Note that we were not able to run the variants with lower enhancement-step accuracy to full precision, as they took too long to converge.)

We also show that CoGenT is fairly robust to selection of regularization parameter τ . We recover a 100–sparse signal of length 2000 from 500 Gaussian measurements, corrupted by AWGN $\sigma = 0.05$. We varied τ by various powers of 2 about its optimal value τ^* , which is the ℓ_1

³Full correction was implemented using CVX [52]

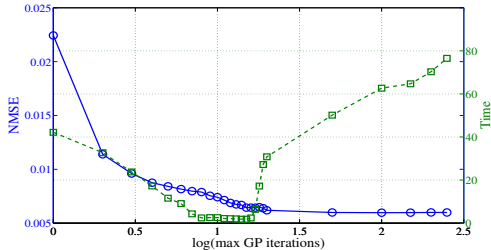


Fig. 2: CoGenT performance as the number of steps in the inner enhancement phase is varied.

norm of the true signal. Note that the NMSE does not change dramatically, and is in fact quite insensitive to τ when τ is greater than τ^* .

Table II shows that the NMSE does not drastically increase, even when τ is made very large. We varied τ as $\tau^* \times 2^t$, for different t , τ^* being the ℓ_1 norm of the true signal.

t	-2	-1	0	1	2	3	4
NMSE	0.172	0.131	0.039	0.057	0.058	0.059	0.063

TABLE II: NMSE for sparse recovery with $\tau = 2^t \tau^*$ for various t .

We next compare CoGenT with some other *greedy* methods for solving ℓ_1 norm constrained problems: CoSaMP [33], Subspace Pursuit [34], and GraDes [53]⁴. We consider a sparse vector of length $p = 20000$ with $s = 1000$ nonzeros randomly chosen, with $n = 5000$ noisy Gaussian measurements, with $\sigma = 0.05$. All codes were run for a maximum of 1000 iterations, with a convergence tolerance of 10^{-4} . Results are averaged over 5 independent trials. Table III shows that GraDes is the fastest, but with a poor solution quality. CG is fast, but with a lack of enhancement and truncation steps, the NMSE is still an order of magnitude worse than CoGenT and SP. Only SP has an NMSE comparable to that of CoGenT, but is much slower. Again, we set $\tau = \|\mathbf{x}\|_1$ for CoGenT and CG, while the other algorithms require the true signal sparsity, which we supply as a parameter.

Fig. 3 shows a comparison of solution quality among the same methods. As a performance metric, we used the mean square error between the true and predicted vectors. We performed 10 independent trials, setting Φ in each trial to be a 3000×10000 matrix, with reference solution \mathbf{x}^* chosen to have $s = 300$ nonzeros, randomly assigned. Observations \mathbf{y} were corrupted with

⁴All codes were obtained directly from the Internet, and were used without modification

Method	Time (seconds)	NMSE
CoSaMP	1479.9	1.5584
SP	3601.1	0.0488
CG	456.96	0.2185
GraDes	405.80	1.0605
CoGenT	1041.6	0.0436

TABLE III: Timing comparisons for CG, CoGenT, Subspace Pursuit (SP), CoSaMP and GraDes.

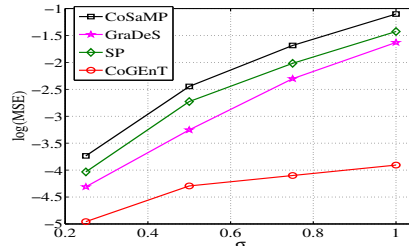


Fig. 3: Comparison of solution quality obtained by different methods.

AWGN with standard deviation σ in the range $[0, 1]$. For CoGenT and CG, we chose $\tau := \|\mathbf{x}^*\|_1$. For CoSaMP, GraDeS and Subspace Pursuit methods, we set $s = 300$, the known sparsity level of the optimal signal. CoGenT performs better at all levels of noise, we believe due to the flexibility of the atomic-constrained formulation, as opposed to a hard limit on the number of basis elements.

B. Overlapping Group Lasso

In group-sparse variants of (13) we seek vectors \mathbf{x} such that $\Phi \mathbf{x} \approx \mathbf{y}$ for given Φ and \mathbf{y} , such that the support of \mathbf{x} consists of a small number of predefined groups of the coefficients. We denote each group by $G \subset \{1, 2, \dots, p\}$ and denote the full collection of groups by \mathcal{G} . CG and CoGenT do not require replication of variables, as is done in prox-linear algorithms [5], [7]. The atom selection step (Step 4 in Algorithm 1) amounts to the following operation:

$$\begin{aligned} \hat{G} &= \arg \max_{G \in \mathcal{G}} \|\llbracket \nabla(f(\mathbf{x}_t)) \rrbracket_G\|, \\ [\mathbf{a}_{t+1}]_{\hat{G}} &= -\llbracket \nabla f(\mathbf{x}_t) \rrbracket_{\hat{G}} / \|\llbracket \nabla f(\mathbf{x}_t) \rrbracket_{\hat{G}}\|, \\ [\mathbf{a}_{t+1}]_i &= 0 \text{ for } i \notin \hat{G}. \end{aligned}$$

We compare the performance of CoGenT with an accelerated proximal point (PP) approach [23] that uses variable replication. We considered M group sparse signals with $\lfloor M/10 \rfloor$ groups chosen to be active in the reference solution, where each group has size 50. The groups are ordered in linear fashion with the last 30 indices of each group overlapping with the first 30 of

the next group. We then took $n = \lceil p/2 \rceil$ measurements with a Gaussian sensing matrix Φ , with AWGN of standard deviation $\sigma = 0.1$ added to the observations. Table IV shows runtimes for the two approaches. We set the maximum iterations to be $2n$ and the tolerance to be 10^{-5} . We searched for τ (CoGenT) and λ (prox) over a grid, and choose the values that yield best MSE performance.

M	True Dimension	Replicated Dimension	time CoGenT	time PP
100	2030	5000	15	22
1000	20030	50000	211	462
1200	24030	60000	359	778
1500	30030	75000	575	1377
2000	40030	100000	852	2977

TABLE IV: Recovery times (in seconds) for CoGenT and prox-linear methods applied to a synthetic overlapping group-sparse problem.

C. Matrix Completion

In low-rank matrix completion, the atoms are rank-one matrices and the observations are individual elements of the matrix. If (\mathbf{u}, \mathbf{v}) are the first left and right singular vectors of $-\nabla f_t$, the solution of Step 4 in Algorithm 1 is $\mathbf{a}_{t+1} = \mathbf{u}\mathbf{v}^T$. The cost of finding only the top singular vectors in the gradient matrix is smaller than the cost of a full SVD by a factor about equal to the smaller dimension of the matrix.

We compared CoGenT with Optspace [26] and SET [27], on matrices of dimension $m \times \lceil \frac{4m}{3} \rceil$ with rank $\max\{3, \lceil \frac{n}{100} \rceil\}$. The matrices were randomly generated as UV^T , with U and V obtained by orthogonalizing random Gaussian matrices of appropriate size. We sampled 20% of the matrix elements and ran all methods until convergence (with a maximum of 5000 iterations and tolerance 10^{-4}). From Fig. 4, we see that CoGenT is faster than SET as the matrix size increases. In fact, SET does not scale well for larger sizes, a regime where CoGenT is still a viable option because of its lower computational cost. Optspace is typically faster, but since it is an alternating minimization method, it may be attracted to local minima. (Recent results have shown that alternating minimization approaches do converge to the global optimum, provided they are initialized appropriately [54].) In terms of reconstruction error, Optspace typically yielded slightly higher error rates compared to SET and CoGenT (see Table V).

V. EXPERIMENTS: NOVEL APPLICATIONS

We now report on the application of CoGenT to recovery problems in several novel areas of application.

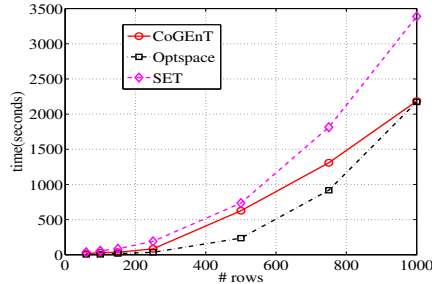


Fig. 4: Speed comparison for Matrix Completion. Results are averaged over 10 trials

# rows	SET	Optspace	CoGenT
60	0.3529	0.4828	0.3518
100	0.1935	0.2969	0.1933
150	0.1524	0.1821	0.1506
250	0.0824	0.1214	0.0817
500	0.0367	0.0493	0.0363
750	0.0247	0.0282	0.0244
1000	0.0184	0.0310	0.0184

TABLE V: MSE $\times 1000$ for the Matrix Completion methods considered. Note that alternating minimization (Optspace) yields higher errors than the other methods.

In some cases, CoGenT and CG are the only practical approaches for solving these problems, while in others, the fact that the signal to be recovered has an “atomic” representation allows CoGenT to be used for recovery.

A. Tensor Completion

Recovery of low-rank tensor approximations arises in applications ranging from multidimensional signal processing to latent-factor models in machine learning [19]. Here, we consider the recovery of symmetric orthogonal tensors from incomplete measurements using CoGenT. We seek a tensor T of the form $T = \sum_{i=1}^r c_i [\otimes \mathbf{u}_i]$, where $\otimes \mathbf{u}$ indicates an t -fold tensor product of a vector $\mathbf{u} \in \mathbb{R}^p$ such that $\|\mathbf{u}\| = 1$. We obtain partial measurements of this tensor of the form $y = \mathcal{M}(T)$, where $\mathcal{M}(\cdot)$ is a *masking operator* that reveals a certain subset of the entries of the tensor. We formulate this problem in an atomic norm setup, wherein the objective function (which captures fidelity to the observations) is $f(T) := \frac{1}{2} \|y - \mathcal{M}(T)\|^2$. The atomic set has the form

$$\mathcal{A} = \{\otimes \mathbf{u} : \mathbf{u} \in \mathbb{R}^p, \|\mathbf{u}\|_2 = 1\}.$$

In applying CoGenT to this problem, the greedy step requires calculation of the symmetric rank-one tensor that best approximates the gradient of the loss function. This calculation can be performed efficiently using power iterations [19]. We implement a backward step

based on basis reoptimization and thresholding (Algorithm 3), where the new basis is obtained from a tensor decomposition, computed via power iterations.

Next, we describe and interpret our numerical experiments. We consider randomly generated orthogonally decomposable tensors of order 3 and rank $r = 3$ of the form $\mathbf{x}^* = \sum_{i=1}^3 c_i v_i^{\otimes 3}$ in all our experiments. The components v_i are chosen by picking random orthonormal sets of vectors in \mathbb{R}^n . In our experiments we vary the dimension of the tensor from $n = 20$ to $n = 60$. Each entry of the tensor is revealed with a specified probability p . We vary the sampling fraction defined as the fraction m/n^3 , where m is the (expected) number of revealed entries. We conduct a number of trials for each pair of tensor size (n) and sampling fraction. In each trial, we declare recovery to be successful if the difference between the true tensor and the recovered tensor (in Euclidean norm) is less than 10^{-4} .

Our experiments compare two approaches. The first approach involves a matricization approach described in [55]–[57], solved using standard a matrix completion approach, implemented in Matlab. The second approach uses CoGenT, making use of backward steps, with forward steps computed using power iterations. The parameter τ as always is set to be the ℓ_1 norm of the true coefficients of the solution.

In Fig. 5, we fix the tensor size at $n = 20$ and plot the empirical probability of success as a function of the sampling fraction, using 20 trials per choice of sampling fraction. Our tensor atomic-norm approach substantially outperforms the matrix unfolding approach. In Fig. 6 we plot the phase transition plots for the two approaches. The x axis we shows the sampling fraction, while the y axis shows the value of n . For each coordinate square, we conduct 10 trials, and plot the empirical probability of success in grayscale, with white representing 1 and black representing 0. We observe that the atomic-norm approach substantially outperforms the matrix unfolding based approach. For instance, for $n = 50$, the matricization approach is unable to reliably recover tensors with sampling fractions below 0.45, whereas the atomic norm approach reliably recovers the same even at sampling fractions of 0.1 (the lowest tried in this set of experiments). It seems that the atomic-norm formulation is more powerful than the matricization approach, and that CoGenT is effective in solving it.

B. Moment Problems in Signal Processing

Consider a continuous time signal

$$\phi(t) = \sum_{j=1}^k c_j \exp(i2\pi f_j t),$$

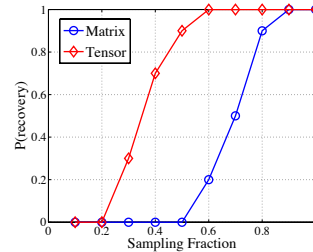


Fig. 5: Comparison of success probabilities for tensors of size $n = 20$.

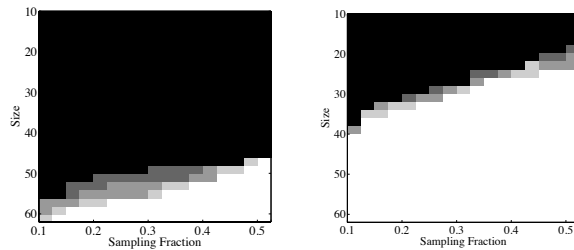


Fig. 6: Phase transition plots based on matricized nuclear norm (left) and atomic norm (right) minimization. White indicates success and black indicates failure in recovery.

for frequencies $f_j \in [0, 1]$, $j = 1, 2, \dots, k$ and coefficients $c_j > 0$, $j = 1, 2, \dots, k$. In many applications of interest, $\phi(t)$ is sampled at times $S := \{t_i\}_{i=1}^n$ giving an observation vector $\mathbf{x} := [\phi(t_1), \phi(t_2), \dots, \phi(t_n)] \in \mathbb{C}^n$. The observed information is therefore

$$\mathbf{x} = \sum_{j=1}^k c_j a(f_j),$$

where

$$a(f_j) = [e^{i2\pi f_j t_1}, e^{i2\pi f_j t_2}, \dots, e^{i2\pi f_j t_n}]^T.$$

Finding the unknown coefficients c_j and frequencies f_j from \mathbf{x} is a challenging problem in general. A natural convex relaxation, analyzed in [12], is obtained by setting $\Phi = I$ in (8) and defining the atoms to be $a(f)$ for $f \in [0, 1]$, a set of infinite cardinality.

The main technical issue in applying CoGenT to this problem is the greedy atom selection step (Step 4 of Algorithm 1), which requires us to find the maximum modulus of a trigonometric polynomial on the unit circle. This operation can be formulated as a semidefinite program [58], but since SDPs do not scale well to high dimensions [12], this approach has limited appeal. In our implementation of CoGenT, we form a discrete grid of frequency values, starting with an initial grid of equally spaced frequencies, refined between iterations by adding

new frequencies midway between each pair of selected frequencies. This approach differs from [12] in that although the initialization is via a grid of frequencies, the ability to refine the grid on a per-iteration basis allows us to achieve much higher precision using fewer grid points. The presence of the backward step in CoGenT means that the method can discard coarse grid points previously selected in favor of better grid points added in later iterations. This also means that the initialization can be quite coarse, another advantage over [12].

By controlling the discretization in this way, we are essentially controlling and refining the inexactness of the forward step (as captured by (11)). Indeed, the accuracy required in (11) can provide guidance for the adaptive discretization process. Step 4 simply selects an atom $a(f)$ corresponding to the frequency f in the current grid that forms the most negative inner product with the gradient of the loss function.

Our implementation of the backward step for this problem has two parts. Besides performing Algorithm 2 to remove multiple uninteresting frequencies, we include a heuristic for merging nearby frequencies, replacing multiple adjacent spikes by a single spike, when it does not degrade the objective too much to do so. Fig. 7 compares the performance of CoGenT with that of standard CG on a signal with ten uniformly randomly chosen frequencies in $[0, 1]$. We take samples at 300 timepoints of a signal of length 1000, corrupted with AWGN with standard deviation .01. The left figure in Fig. 7 shows the signal recovered by CoGenT, indicating that all but the smallest of the ten spikes were recovered accurately. The critical role played by the backward step can be seen by contrasting these results with those reported for CG in the right figure of Fig. 7, where many spurious frequencies appear.

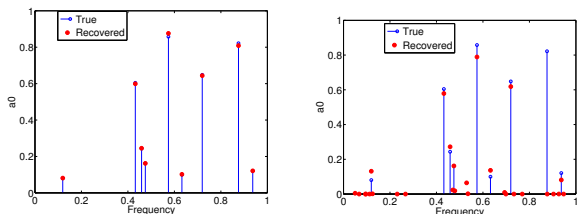


Fig. 7: CoGenT and CG for off-grid compressed sensing. Blue spikes and circles represent the reference solution, and red circles are those estimated by the algorithms.

We compared CoGenT to the SDP formulation as explained in [12]. Although the SDP solves the problem exactly, it does not scale well to large dimensions, as we show in the timing comparisons of Fig. 8. The instances

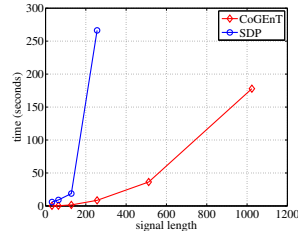
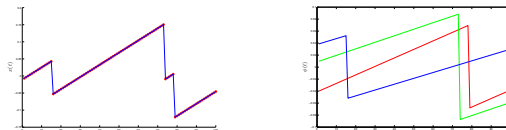


Fig. 8: Speed comparison with SDP. The SDP formulation does not scale well.



(a) The true signal (blue) is a superposition of sawtooth functions. Red dots show samples acquired. (b) Sawtooth components recovered by CoGenT.

Fig. 9: Recovering sawtooth components by sampling. (Best seen in color)

were generated as follows: For a particular signal length p , we randomly choose 5 frequencies to be active, choosing values from a uniform $(0, 1]$ distribution. We obtain $p/4$ noisy measurements with $\sigma = 0.1$. We run CoGenT with $2n$ iterations and a tolerance of 10^{-10} .

The formulation above can be generalized to include signals that are a conic combination of a few arbitrary functions of the form $\phi(t, \alpha_i)$.

- Bessel and Airy functions form natural signal ensembles that arise as solutions to differential equations in physics. As an example, letting $J_r(t)$ denote Bessel functions of the first kind, we have

$$\phi(t; \alpha_1, \alpha_2, \alpha_3) = J_{\alpha_1} \left(\frac{t}{\alpha_2} - \alpha_3 \right),$$

where $\alpha_1, \alpha_2, \alpha_3 \in \mathbb{R}_+$. Here, each atom is defined by a specific choice of the triple $(\alpha_1, \alpha_2, \alpha_3)$, leading to an atomic set \mathcal{A} with infinite cardinality.

- Triangle and sawtooth waves. Consider for instance the sawtooth functions:

$$\phi(t; \alpha_1, \alpha_2) = \frac{t}{\alpha_1} - \left\lfloor \frac{t}{\alpha_1} \right\rfloor - \alpha_2,$$

where $\alpha_1, \alpha_2 \in \mathbb{R}_+$. Each atom is defined by a specific choice of (α_1, α_2) . Fig. 9 shows successful recovery of a superposition of sawtooth functions from a limited number of samples.

- Ricker wavelets arise in seismology applications, with the atoms characterized by $\sigma > 0$:

$$\phi(t; \sigma) = \frac{2}{\sqrt{3\sigma\pi^{\frac{1}{4}}}} \left(1 - \frac{t^2}{\sigma^2}\right) \exp\left(-\frac{t^2}{2\sigma^2}\right).$$

- Gaussians, characterized by parameters μ and σ :

$$\phi(t; \mu, \sigma) = \frac{1}{\sqrt{2\pi}\sigma} \exp\left(-\frac{(t - \mu)^2}{2\sigma^2}\right).$$

Estimating Gaussian mixtures from sampled data is a much-studied problem in machine learning.

The key ingredient in solving these problems within the atomic norm framework is efficient (approximate) solution of the atom selection step. In some cases, this can be done in closed form, whereas for all the signals mentioned above, approximate solutions can be obtained via adaptive discretization.

C. OSCAR

The regularizer for the Octagonal Shrinkage and Clustering Algorithm for Regression (OSCAR) method is defined for $\mathbf{x} \in \mathbb{R}^p$ as follows:

$$\|\mathbf{x}\|_1 + c \sum_{j=1}^p \sum_{k=1}^j \max\{|\mathbf{x}_j|, |\mathbf{x}_k|\}$$

In [18], the authors show that this indeed can be expressed as an atomic norm, and also give an efficient method to find the next atom to add in the forward greedy step. We compared CoGenT for OSCAR with the proximal point based scheme [59], of which OSCAR is a special case. (For a comparison of different prox-based methods, we refer to the interested reader to [60].) We considered a length 5000 vector x of the following form:

$$a = \theta_a + \zeta_a, \quad b = \theta_b + \zeta_b, \quad c = \theta_c + \zeta_c \quad d = \theta_d + \zeta_d$$

where the ζ are vectors of length 20 with *i.i.d.* Gaussian entries, and $\theta \sim \mathcal{U}[-1, 1]$. In MATLAB notation, $x(1 : 20) = a$, $x(301 : 320) = b$, $x(801 : 820) = c$, $x(1001 : 1020) = d$. We obtained 500 Gaussian measurements and corrupted them with varying amounts of noise σ . We allowed both methods to run for at most 1000 iterations, with a convergence tolerance of 10^{-6} . Fig. 10 shows the results we obtained, in terms of MSE $\|\hat{\mathbf{x}} - \mathbf{x}\|_2^2/1000$. We do not report timing results in this case, since we were comparing our MATLAB code with C code. However, the standard CG method has been observed to be faster than prox-based methods, so it is reasonable to expect CoGenT to be faster as well, when implemented appropriately.

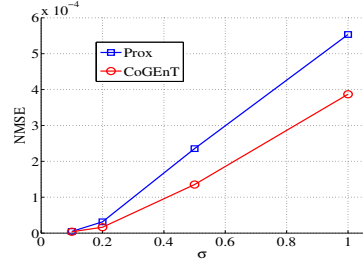


Fig. 10: Comparison between CoGenT and proximal-point methods for solving the OSCAR problem. We found CoGenT to be more robust to noise.

VI. RECONSTRUCTION AND DECONVOLUTION

The deconvolution problem involves recovering a signal of the form $\mathbf{x} = \mathbf{x}^1 + \mathbf{x}^2$ from observations \mathbf{y} via a sensing matrix Φ , where \mathbf{x}^1 and \mathbf{x}^2 can be expressed compactly with respect to different atomic sets \mathcal{A}_1 and \mathcal{A}_2 . We mentioned several instances of such problems in Section I. Adopting the optimization-driven approach outlined in Section I, we arrive at the following convex optimization formulation:

$$\begin{aligned} & \underset{\mathbf{x}^1, \mathbf{x}^2}{\text{minimize}} && \frac{1}{2} \|\mathbf{y} - \Phi(\mathbf{x}^1 + \mathbf{x}^2)\|^2 \\ & \text{subject to} && \|\mathbf{x}^1\|_{\mathcal{A}_1} \leq \tau_1 \text{ and } \|\mathbf{x}^2\|_{\mathcal{A}_2} \leq \tau_2. \end{aligned}$$

Algorithm 1 can be extended to this situation, as we describe informally now. Each iteration starts by choosing an atom from \mathcal{A}_1 that nearly minimizes its inner product with the gradient of the objective function with respect to \mathbf{x}^1 ; this is the forward step with respect to \mathcal{A}_1 . One then performs a backward step for \mathcal{A}_1 . Next follows a similar forward step with respect to \mathcal{A}_2 , followed by a backward step for \mathcal{A}_2 . We then proceed to the next iteration, unless convergence is flagged. Note that the backward steps are taken only if they do not deteriorate the objective function beyond a specified threshold. The procedure is repeated until a termination condition is satisfied.

It is important to note that the method outlined above is a heuristic extension of CoGenT, and the convergence properties we have proved do not directly translate to this setting. Nonetheless, we show below that the method yields good empirical results.

In our first example, we consider the standard recovery of sparse + low rank matrices. We consider a matrix of size 50×50 , which is a sum of a random rank 4 matrix (generated by truncating the SVD of a random Gaussian matrix) and a sparse matrix with 100 randomly chosen indices with standard normally distributed entries. The sets \mathcal{A}_1 and \mathcal{A}_2 are defined in the usual way for these

types of matrices. Fig. 11 shows that CoGenT recovers the components accurately. Note that the goal here is not to show that CoGenT outperforms other methods for Robust PCA, but rather to demonstrate that even this problem can be solved with a variant of CoGenT. Along similar lines, we note that CoGenT can be used to deconvolve spikes and sinusoids, or group sparse and sparse signals [22].

We consider now a novel application: *graph deconvolution*. To state this problem formally, consider two simple, undirected weighted graphs $\mathcal{G}_1 = (V, W_1)$ and $\mathcal{G}_2 = (V, W_2)$ where V represents a (common) vertex set and W_1, W_2 are the weighted adjacency matrices, with superposition $W = W_1 + W_2$. Problems of this form are of interest in *covariance estimation*: W_1 and W_2 may correspond to covariance matrices of random vectors X_1 and X_2 , and from samples of $X = X_1 + X_2$, one may wish to recover the covariances W_1 and W_2 .

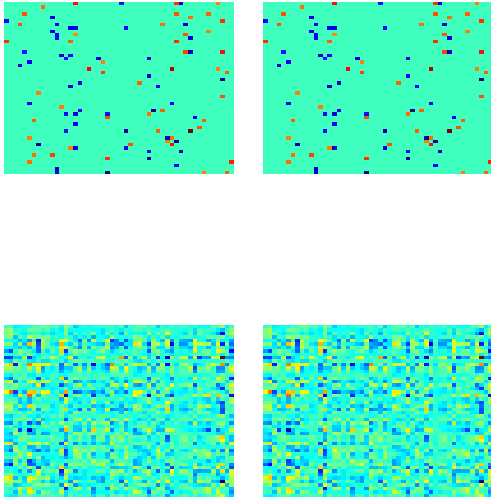


Fig. 11: Recovery of a sparse + low rank matrix. The left column shows true components, and the right column shows recovered components. The top row shows the sparse part and the bottom row shows the low-rank part. Error in each recovered component is at most 10^{-7} .

We consider a graph of $|V| = 50$ nodes in which \mathcal{G}_1 and \mathcal{G}_2 are each restricted to a specific family of graphs \mathfrak{T}_1 and \mathfrak{T}_2 , respectively, with the following properties.

- \mathfrak{T}_1 is the class of all tree-structured graphs on 50 nodes. Note that the only information we exploit here is the fact that \mathcal{G}_1 is tree structured. Neither the

edges of the tree nor the edge weights are known.

- \mathfrak{T}_2 is the class of two-dimensional 5×10 grid graphs on 50 nodes. The nodes of the graph are known up to a cyclic permutation. Once again, neither the edges of the graph nor the corresponding weights are known. The only information available is that one of the 50 cyclic permutations of the nodes yields the desired grid-structured graph.

For set \mathfrak{T}_1 , we define \mathcal{A}_1 to be the set of all matrices with Frobenius norm 1, whose nonzero structure is the adjacency matrix of a tree.⁵ For the set \mathfrak{T}_2 we define \mathcal{A}_2 as follows. Let $\mathcal{P} \subseteq \mathbb{R}^{n \times n}$ denote the set of all permutation matrices corresponding to the cyclic permutations (that is, permutations in the cyclic group of order n). Let $\mathcal{G}(p, q)$ (with $pq = n$) denote the set of all weighted adjacency matrices (of unit Frobenius norm) of $p \times q$ grid graphs with a fixed canonical labeling of the nodes. The atomic set \mathcal{A}_2 is the set of weighted adjacency matrices for cyclic permutations of all these adjacency matrices.

Given these definitions, and assuming that we observe the full matrices, we state this deconvolution problem as:

$$\begin{aligned} & \underset{X_1, X_2}{\text{minimize}} && \frac{1}{2} \|W - X_1 - X_2\|^2 \\ & \text{subject to} && \|X_1\|_{\mathcal{A}_1} \leq \tau_1 \text{ and } \|X_2\|_{\mathcal{A}_2} \leq \tau_2. \end{aligned}$$

We need to compute the dual atomic norms to implement the forward steps in CoGenT. The variational descriptions of the dual atomic norms are given by:

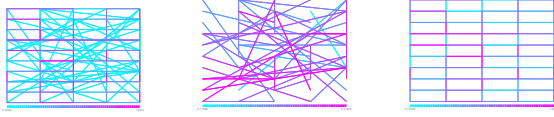
$$\|Y\|_{\mathcal{A}_i}^* = \max_{Z \in \mathcal{A}_i} [\text{trace}(ZY)]$$

For \mathcal{A}_1 , the dual norm essentially amounts to computation of a maximum weight spanning tree, while for \mathcal{A}_2 , the dual norm can be computed in a straightforward way by sweeping through the n possible permutations of the grid graph to solve:

$$\|Y\|_{\mathcal{A}_2}^* = \max_{P \in \mathcal{P}, \|\mathcal{G}(p, q)\|_F \leq 1} \text{trace}(P' \mathcal{G}(p, q) P Y).$$

Our problem instances are generated as follows. We created a random tree by generating a random (symmetric) matrix with entries distributed as $\mathcal{U}[0, 1]$, and extracting its maximum weight spanning tree. The grid component was also chosen with similarly chosen random weights. The resulting graphs were then superposed and then randomly permuted. We implemented the deconvolution variant of CoGenT with backward steps as described in Algorithm 2. Results are shown in Fig. 12. CoGenT achieves exact recovery; that is, the edges as

⁵We learned of the construction of tree-structured norms from James Saunderson, and express our gratitude for this insight.



(a) True signal is a superposition of a weighted tree and a weighted grid graph. (b) Tree component, recovered by CoGenT. (c) Grid graph component, recovered by CoGenT.

Fig. 12: Recovering constituent graph components from a superposition of weighted graphs. Edge weights are color-coded, with darker colors representing higher weights. CoGenT correctly deconvolves the graph into its constituent components. (Best seen in color)

well as the edge weights of the constituent graphs are correctly recovered.

VII. CONCLUSION

We introduced CoGenT, a greedy scheme for recovering signals that are representable as a linear combination of a few fundamental elements from some basis. We showed that our method is efficient and broadly applicable, and enjoys the same theoretical convergence properties as conditional gradient. We have described results obtained on a variety of interesting problems, including compressed sensing, matrix completion, moment problems and deconvolution.

APPENDIX

Theorem III.2 is (except for a minor difference in the upper bounds on η) a true generalization of Theorem III.1, in that we recover the statement of Theorem III.1 by setting $\omega = 0$ in Theorem III.2. Likewise, the *proof* of Theorem III.1 can be obtained by setting $\omega = 0$ in Theorem III.2, so we prove only the latter result here.

A. Proof of Theorem III.2

Denote $f_t := f(\mathbf{x}_t)$, $\tilde{f}_t := f(\tilde{\mathbf{x}}_t)$, and $f_t^{FW} := f(\mathbf{x}_{t-1} + \gamma_t(\tau \mathbf{a}_t - \mathbf{x}_{t-1}))$. We have from the algorithm description that

$$f_{t+1} \leq \eta f_t + (1 - \eta) f_{t+1}^{FW}.$$

For $\gamma \in [0, 1]$, we define

$$\mathbf{x}_t(\gamma) := (1 - \gamma)\mathbf{x}_t + \gamma\tau\mathbf{a}_{t+1}.$$

Because Step 6 of Algorithm 1 chooses the value of γ optimally, we have $f_{t+1}^{FW} = f(\mathbf{x}_t(\gamma_{t+1})) \leq f(\mathbf{x}_t(\gamma))$, for all $\gamma \in [0, 1]$, and so

$$\begin{aligned} f_{t+1} &\leq \eta f_t + (1 - \eta) f_{t+1}^{FW} \\ &\leq \eta f_t + (1 - \eta) f(\mathbf{x}_t(\gamma)) \\ &\leq \eta f_t + (1 - \eta) [f_t + \nabla f(\mathbf{x}_t)^T (\mathbf{x}_t(\gamma) - \mathbf{x}_t)] + \\ &\quad (1 - \eta) \left[\frac{L}{2} \|\mathbf{x}_t(\gamma) - \mathbf{x}_t\|^2 \right] \quad (\text{by definition of } L) \\ &= f_t + (1 - \eta) [\nabla f(\mathbf{x}_t)^T ((1 - \gamma)\mathbf{x}_t + \gamma\tau\mathbf{a}_{t+1} - \mathbf{x}_t)] + \\ &\quad (1 - \eta) \left[\frac{L}{2} \|(1 - \gamma)\mathbf{x}_t + \gamma\tau\mathbf{a}_{t+1} - \mathbf{x}_t\|^2 \right] \\ &= f_t + (1 - \eta) [\gamma \nabla f(\mathbf{x}_t)^T (\tau\mathbf{a}_{t+1} - \mathbf{x}_t)] + \\ &\quad (1 - \eta) \left[\frac{L\gamma^2}{2} \|\tau\mathbf{a}_{t+1} - \mathbf{x}_t\|^2 \right] \\ &\leq f_t + (1 - \eta) [\gamma(1 - \omega) \nabla f(\mathbf{x}_t)^T (\mathbf{x}^* - \mathbf{x}_t)] + \\ &\quad (1 - \eta) [2\gamma^2 LR^2 \tau^2] \quad (\text{see below}) \\ &\leq f_t + (1 - \eta) [\gamma(1 - \omega)(f_* - f_t) + 2\gamma^2 LR^2 \tau^2]. \end{aligned} \tag{14}$$

The last inequality follows from convexity of the objective function. The second-last inequality uses two results. First, note that the solution \mathbf{x}^* can be expressed as follows:

$$\mathbf{x}^* = \sum_{\mathbf{a} \in \mathcal{A}} c_{\mathbf{a}}^* \mathbf{a}, \quad \text{for } c_{\mathbf{a}}^* \geq 0 \text{ with } \sum_{\mathbf{a} \in \mathcal{A}} c_{\mathbf{a}}^* \leq \tau.$$

We therefore have

$$\begin{aligned} &\langle \nabla f(\mathbf{x}_t), \mathbf{x}^* - \mathbf{x}_t \rangle \\ &= \left\langle \nabla f(\mathbf{x}_t), \left(\sum_{\mathbf{a} \in \mathcal{A}} c_{\mathbf{a}}^* \mathbf{a} \right) - \mathbf{x}_t \right\rangle \\ &\geq \left(\sum_{\mathbf{a} \in \mathcal{A}} c_{\mathbf{a}}^* \right) \min_{\mathbf{a} \in \mathcal{A}} \langle \nabla f(\mathbf{x}_t), \mathbf{a} \rangle - \langle \nabla f(\mathbf{x}_t), \mathbf{x}_t \rangle \\ &\geq \min_{\mathbf{a} \in \mathcal{A}} \langle \nabla f(\mathbf{x}_t), \tau \mathbf{a} - \mathbf{x}_t \rangle \\ &\geq \frac{1}{1 - \omega} \langle \nabla f(\mathbf{x}_t), \tau \mathbf{a}_{t+1} - \mathbf{x}_t \rangle, \end{aligned}$$

by the definition of \mathbf{a}_{t+1} in (11) and noting that $\min_{\mathbf{a} \in \mathcal{A}} \langle \nabla f(\mathbf{x}_t), \mathbf{a} \rangle \leq 0$. Second, we use the definition of R together with $\|\mathbf{x}_t\|_{\mathcal{A}} \leq \tau$ and $\mathbf{a}_{t+1} \in \mathcal{A}$ to deduce

$$\|\tau \mathbf{a}_{t+1} - \mathbf{x}_t\| \leq \tau (\|\mathbf{a}_{t+1}\| + \|\mathbf{x}_t/\tau\|) \leq 2\tau R,$$

which we can use to bound the squared-norm term. By subtracting f^* from both sides of (14), and defining

$$\delta_t := f(\mathbf{x}_t) - f^*, \quad (15)$$

we obtain that

$$\delta_{t+1} \leq [1 - \gamma(1 - \eta)(1 - \omega)] \delta_t + 2(1 - \eta)LR^2\gamma^2\tau^2, \quad (16)$$

for all $\gamma \in [0, 1]$. This inequality implies immediately that $\{\delta_t\}_{t=0,1,2,\dots}$ is a decreasing sequence, since $\gamma = 0$ is always a valid choice in (16).

Note that $\delta_0 = f_0 - f_* = D$. For the first iteration $t = 0$, set $\gamma = 1$ in (16) to obtain a further bound on δ_1 :

$$\delta_1 \leq [\eta + \omega(1 - \eta)]D + 2(1 - \eta)LR^2\tau^2 = \tilde{C}_1.$$

For subsequent iterations $t \geq 1$, we consider the following choice of γ :

$$\tilde{\gamma}_t := \frac{\delta_t}{2\tilde{C}_1}.$$

By monotonicity of $\{\delta_t\}$ and the bound above on δ_1 , we have $\tilde{\gamma}_t \leq 1/2$ for all $t \geq 1$. By substituting the choice $\gamma = \tilde{\gamma}_t$ into (16), we obtain

$$\begin{aligned} \delta_{t+1} &\leq \delta_t - \delta_t^2 \frac{(1 - \eta)(1 - \omega)\tilde{C}_1 - (1 - \eta)LR^2\tau^2}{2\tilde{C}_1^2} \\ &= \delta_t - \frac{\delta_t^2}{\tilde{C}}. \end{aligned} \quad (17)$$

The denominator of \tilde{C} is positive because $\eta \in (0, 1/3]$ and $\omega \in (0, 1/4]$ together imply that

$$(1 - \omega)\tilde{C}_1 - LR^2\tau^2 > 2(1 - \omega)(1 - \eta)LR^2\tau^2 - LR^2\tau^2 \geq 0.$$

Note too that

$$\tilde{C} = \frac{2\tilde{C}_1^2}{(1 - \eta)((1 - \omega)\tilde{C}_1 - LR^2\tau^2)} > 2\tilde{C}_1,$$

so that $\delta_1 \leq \tilde{C}/2$. An argument from [49, Lemma 2.1] yields the result. Since $\delta_1 \leq \tilde{C}/2$, the bound (12) holds for $t = 1$. Since $\{\delta_t\}$ is a decreasing sequence, we have $\delta_t \leq \tilde{C}/2$ for all $t \geq 1$. For the inductive step, assume that (12) holds for some $t \geq 1$. Since the right-hand side of (17) is an increasing function of δ_t for all $\delta_t \in (0, \tilde{C}/2)$, this quantity can be upper-bounded by substituting the upper bound $\tilde{C}/(t + 1)$ for δ_t , to obtain

$$\begin{aligned} \delta_{t+1} &\leq \delta_t - \frac{\delta_t^2}{\tilde{C}} \leq \frac{\tilde{C}}{(t + 1)} - \frac{\tilde{C}}{(t + 1)^2} \\ &= \frac{\tilde{C}t}{(t + 1)^2} = \frac{\tilde{C}t(t + 2)}{(t + 1)^2(t + 2)} \leq \frac{\tilde{C}}{t + 2}, \end{aligned}$$

establishing the inductive step and completing the proof.

REFERENCES

- [1] V. Chandrasekaran, B. Recht, P. A. Parrilo, and A. S. Willsky, "The convex geometry of linear inverse problems," *Foundations of Computational Mathematics*, vol. 12, no. 6, pp. 805–849, 2012.
- [2] E. J. Candès, J. Romberg, and T. Tao, "Robust uncertainty principles: Exact signal reconstruction from highly incomplete frequency information," *IEEE Transactions on Information Theory*, vol. 52, no. 2, pp. 489–509, 2006.
- [3] E. J. Candès and B. Recht, "Exact matrix completion via convex optimization," *Foundations of Computational Mathematics*, vol. 9, no. 6, pp. 717–772, 2009.
- [4] B. Recht, M. Fazel, and P. A. Parrilo, "Guaranteed minimum-rank solutions of linear matrix equations via nuclear norm minimization," *SIAM Review*, vol. 52, no. 3, pp. 471–501, 2010.
- [5] N. S. Rao, R. D. Nowak, S. J. Wright, and N. G. Kingsbury, "Convex approaches to model wavelet sparsity patterns," in *Image Processing (ICIP), 2011 18th IEEE International Conference on*. IEEE, 2011, pp. 1917–1920.
- [6] F. R. Bach, "Consistency of the group lasso and multiple kernel learning," *Journal of Machine Learning Research*, vol. 9, pp. 1179–1225, 2008.
- [7] L. Jacob, G. Obozinski, and J.-P. Vert, "Group lasso with overlap and graph lasso," in *Proceedings of the 26th Annual International Conference on Machine Learning*. ACM, 2009, pp. 433–440.
- [8] J. Mairal, R. Jenatton, G. Obozinski, and F. Bach, "Convex and network flow optimization for structured sparsity," *The Journal of Machine Learning Research*, vol. 12, pp. 2681–2720, 2011.
- [9] S. Negahban and M. J. Wainwright, "Joint support recovery under high-dimensional scaling: Benefits and perils of l_1 -regularization," *Advances in Neural Information Processing Systems*, vol. 21, pp. 1161–1168, 2008.
- [10] B. A. Turlach, W. N. Venables, and S. J. Wright, "Simultaneous variable selection," *Technometrics*, vol. 47, no. 3, pp. 349–363, 2005.
- [11] N. S. Rao, B. Recht, and R. D. Nowak, "Universal measurement bounds for structured sparse signal recovery," in *International Conference on Artificial Intelligence and Statistics*, 2012, pp. 942–950.
- [12] G. Tang, B. N. Bhaskar, P. Shah, and B. Recht, "Compressive sensing off the grid," in *50th Annual Allerton Conference on Communication, Control, and Computing*. IEEE, 2012, pp. 778–785.
- [13] M. Cheraghchi, A. Karbasi, S. Mohajer, and V. Saligrama, "Graph-constrained group testing," in *2010 IEEE International Symposium on Information Theory Proceedings (ISIT)*. IEEE, 2010, pp. 1913–1917.
- [14] R. Jenatton, J. Mairal, G. Obozinski, and F. Bach, "Proximal methods for hierarchical sparse coding," *Journal of Machine Learning Research*, vol. 12, pp. 2297–2334, 2010.
- [15] S. Chatterjee, A. Banerjee, S. Chatterjee, and A. R. Ganguly, "Sparse group lasso for regression on land climate variables." in *ICDM Workshops*, 2011, pp. 1–8.
- [16] N. Rao, C. Cox, R. Nowak, and T. T. Rogers, "Sparse overlapping sets lasso for multitask learning and its application to fmri analysis," in *Advances in Neural Information Processing Systems*, 2013, pp. 2202–2210.
- [17] H. D. Bondell and B. J. Reich, "Simultaneous regression shrinkage, variable selection, and supervised clustering of predictors with oscar," *Biometrics*, vol. 64, no. 1, pp. 115–123, 2008.
- [18] X. Zeng and M. Figueiredo, "The atomic norm formulation of OSCAR regularization with application to the Frank-Wolfe algorithm," in *Proceedings of the European Signal Processing Conference, Lisbon, Portugal*, 2014.
- [19] A. Anandkumar, R. Ge, D. Hsu, S. M. Kakade, and M. Telgarsky, "Tensor decompositions for learning latent variable models," *The Journal of Machine Learning Research*, vol. 15, no. 1, pp. 2773–2832, 2014.

- [20] M. McCoy, V. Cevher, Q. Dinh, A. Asaci, and L. Baldassarre, "Convexity in source separation: Models, geometry, and algorithms," *Signal Processing Magazine, IEEE*, vol. 31, no. 3, pp. 87–95, 2014.
- [21] A. E. Waters, A. C. Sankaranarayanan, and R. G. Baraniuk, "Sparscs: Recovering low-rank and sparse matrices from compressive measurements," in *Advances in Neural Information Processing Systems*, 2011, pp. 1089–1097.
- [22] A. Jalali, P. D. Ravikumar, S. Sanghavi, and C. Ruan, "A dirty model for multi-task learning," *Advances in Neural Information Processing Systems*, vol. 23, pp. 964–972, 2010.
- [23] S. J. Wright, R. D. Nowak, and M. A. Figueiredo, "Sparse reconstruction by separable approximation," *IEEE Transactions on Signal Processing*, vol. 57, no. 7, pp. 2479–2493, 2009.
- [24] J. A. Tropp and A. C. Gilbert, "Signal recovery from random measurements via orthogonal matching pursuit," *IEEE Transactions on Information Theory*, vol. 53, no. 12, pp. 4655–4666, 2007.
- [25] R. Tibshirani, "Regression shrinkage and selection via the lasso," *Journal of the Royal Statistical Society. Series B (Methodological)*, pp. 267–288, 1996.
- [26] R. Keshavan, A. Montanari, and S. Oh, "Matrix completion from noisy entries," in *Advances in Neural Information Processing Systems*, 2009, pp. 952–960.
- [27] W. Dai and O. Milenkovic, "Set: an algorithm for consistent matrix completion," in *Acoustics Speech and Signal Processing (ICASSP), 2010 IEEE International Conference on*. IEEE, 2010, pp. 3646–3649.
- [28] M. Jaggi, "Revisiting Frank-Wolfe: Projection-free sparse convex optimization," in *Proceedings of the 30th International Conference on Machine Learning*, 2013, pp. 427–435.
- [29] J. C. Dunn, "Rates of convergence for conditional gradient algorithms near singular and nonsingular extremals," *SIAM Journal on Control and Optimization*, vol. 17, no. 2, pp. 187–211, 1979.
- [30] A. Tewari, P. K. Ravikumar, and I. S. Dhillon, "Greedy algorithms for structurally constrained high dimensional problems," in *Advances in Neural Information Processing Systems*, 2011, pp. 882–890.
- [31] M. Dudik, Z. Harchaoui, and J. Malick, "Learning with matrix gauge regularizers," *NIPS Optimization Workshop*, 2011.
- [32] R. M. Freund and P. Grigas, "New analysis and results for the conditional gradient method," preprint arXiv:1307.0873, 2013.
- [33] D. Needell and J. A. Tropp, "CoSaMP: Iterative signal recovery from incomplete and inaccurate samples," *Applied and Computational Harmonic Analysis*, vol. 26, no. 3, pp. 301–321, 2009.
- [34] W. Dai and O. Milenkovic, "Subspace pursuit for compressive sensing signal reconstruction," *IEEE Transactions on Information Theory*, vol. 55, no. 5, pp. 2230–2249, 2009.
- [35] M. Frank and P. Wolfe, "An algorithm for quadratic programming," *Naval Research Logistics Quarterly*, vol. 3, no. 1-2, pp. 95–110, 1956.
- [36] A. Beck and M. Teboulle, "A fast iterative shrinkage-thresholding algorithm for linear inverse problems," *SIAM Journal on Imaging Sciences*, vol. 2, no. 1, pp. 183–202, 2009.
- [37] Y. Nesterov, "Gradient methods for minimizing composite objective functions," *Mathematical Programming, Series B*, 2013, to appear.
- [38] J.-F. Cai, E. J. Candès, and Z. Shen, "A singular value thresholding algorithm for matrix completion," *SIAM Journal on Optimization*, vol. 20, no. 4, pp. 1956–1982, 2010.
- [39] S. Lacoste-Julien, M. Jaggi, M. Schmidt, P. Pletscher *et al.*, "Block-coordinate Frank-Wolfe optimization for structural SVMs," *International Conference on Machine Learning*, pp. 53–61, 2013.
- [40] J. Guélat and P. Marcotte, "Some comments on Wolfe's away step," *Mathematical Programming*, vol. 35, no. 1, pp. 110–119, 1986.
- [41] P. Wolfe, "Convergence theory in nonlinear programming," in *Integer and Nonlinear Programming*, J. Abadie, Ed. Amsterdam: North-Holland, 1970.
- [42] T. Zhang, "Adaptive forward-backward greedy algorithm for learning sparse representations," *IEEE Transactions on Information Theory*, vol. 57, no. 7, pp. 4689–4708, 2011.
- [43] P. Jain, A. Tewari, and I. S. Dhillon, "Orthogonal matching pursuit with replacement," *Advances in Neural Information Processing Systems*, pp. 1215–1223, 2011.
- [44] C. C. Johnson, A. Jalali, and P. D. Ravikumar, "High-dimensional sparse inverse covariance estimation using greedy methods," *International Conference on Artificial Intelligence and Statistics*, pp. 574–582, 2012.
- [45] J. Liu, J. Ye, and R. Fujimaki, "Forward-backward greedy algorithms for general convex smooth functions over a cardinality constraint," in *Proceedings of the 31st International Conference on Machine Learning (ICML-14)*, 2014, pp. 503–511.
- [46] N. Rao, P. Shah, S. Wright, and R. Nowak, "A greedy forward-backward algorithm for atomic norm constrained minimization," in *Acoustics, Speech and Signal Processing (ICASSP), 2013 IEEE International Conference on*. IEEE, 2013, pp. 5885–5889.
- [47] N. Rao, P. Shah, and S. Wright, "Conditional gradient with enhancement and truncation for atomic-norm regularization," in *NIPS Workshop on Greedy Algorithms*, 2013.
- [48] J. Duchi, S. Shalev-Shwartz, Y. Singer, and T. Chandra, "Efficient projections onto the l_1 -ball for learning in high dimensions," in *Proceedings of the 25th International conference on Machine learning*. ACM, 2008, pp. 272–279.
- [49] A. Beck and M. Teboulle, "A conditional gradient method with linear rate of convergence for solving convex linear systems," *Mathematical Methods of Operations Research*, vol. 59, no. 2, pp. 235–247, 2004.
- [50] J. Nocedal and S. Wright, *Numerical Optimization*, 2nd ed. Springer, 2006.
- [51] F. Bach, "Convex relaxations of structured matrix functions," INRIA Paris - Rocquencourt, Technical Report arXiv:1309.3117, September 2013.
- [52] M. Grant, S. Boyd, and Y. Ye, "CVX: Matlab software for disciplined convex programming," 2008.
- [53] R. Garg and R. Khandekar, "Gradient descent with sparsification: an iterative algorithm for sparse recovery with restricted isometry property," in *Proceedings of the 26th Annual International Conference on Machine Learning*. ACM, 2009, pp. 337–344.
- [54] P. Jain, P. Netrapalli, and S. Sanghavi, "Low-rank matrix completion using alternating minimization," in *Proceedings of the forty-fifth annual ACM symposium on Theory of computing*. ACM, 2013, pp. 665–674.
- [55] C. Mu, B. Huang, J. Wright, and D. Goldfarb, "Square deal: Lower bounds and improved relaxations for tensor recovery," in *Proceedings of the 31st International Conference on Machine Learning (ICML-14)*, 2014, pp. 73–81.
- [56] S. Gandy, B. Recht, and I. Yamada, "Tensor completion and low-n-rank tensor recovery via convex optimization," *Inverse Problems*, vol. 27, no. 2, p. 025010, 2011.
- [57] J. Liu, P. Musialski, P. Wonka, and J. Ye, "Tensor completion for estimating missing values in visual data," *Pattern Analysis and Machine Intelligence, IEEE Transactions on*, vol. 35, no. 1, pp. 208–220, 2013.
- [58] B. Dumitrescu, *Positive Trigonometric Polynomials and Signal Processing Applications*. Springer, 2007.
- [59] M. Bogdan, E. van den Berg, W. Su, and E. Candès, "Statistical estimation and testing via the ordered L_1 norm," *arXiv preprint arXiv:1310.1969*, 2013.
- [60] X. Zeng and M. A. Figueiredo, "Solving OSCAR regularization problems by proximal splitting algorithms," *arXiv preprint arXiv:1309.6301*, 2013.